

# Plant Stress Detection by Thermography

Subjects: Plant Sciences

Contributor: Marisa Pérez-Bueno

Leaf and canopy temperature is a valuable indicator of the physiological status of plants, responding to both biotic and abiotic stressors. Thermography, often combined with other imaging sensors and data-mining techniques, is crucial in the implementation of a more automatized, precise and sustainable agriculture.

Keywords: Remote sensing ; proximal sensing ; biotic stress ; plant stress

---

## 1. Introduction

Environmental conditions driven by climate change and infections are great challenges that need to be overcome by modern agriculture. The economic loss in agriculture caused by increasing environmental pressures could reach an annual 0.3% to 0.8% of projected global gross domestic product by the end of the century <sup>[1]</sup>. Moreover, plant diseases are the main cause of the drop in production and economic losses in agriculture worldwide, reaching yield losses of 20 to 30% depending on the crop <sup>[2]</sup>. Current practices and social activities -such as intensified monoculture in large areas, the use of genetically uniform plant varieties and the development of global supply chains and logistic activities- contribute largely to the widespread of plant disease epidemics and rapid pathogen evolution <sup>[3]</sup>.

Plant phenotyping based on imaging techniques is a pertinent approach to quantify the appearance and performance of crops under different environmental conditions while addressing the spatial heterogeneity of crop fields. Therefore, plant phenotyping, applied to precision agriculture, is a valuable tool for the diagnosis and detection of plant stress, even in the absence of symptoms. Optical sensors have been used to study a) the response of plants to pathogens, pests and abiotic stressors; b) to identify primary disease foci; c) to monitor resistance or susceptibility of different plant genotypes to specific stress factors; d) to evaluate the severity of symptoms; e) and to assess plant biomass and yield <sup>[4]</sup>.

Stomatal activity is one of the most important physiological traits for plant growth and development. It plays a crucial role in the carbon and water balance by controlling photosynthesis and transpiration <sup>[5]</sup>. Hence, stomatal conductance to water (gs) is related to yield and to the tolerance of environmental stresses <sup>[6]</sup> and correlates strongly with leaf temperature <sup>[7][8][9]</sup>. Thermal long-wave infrared (TIR) cameras (or simply thermal cameras) are calibrated sensors able to record emitted radiation in the thermal range (8–14  $\mu\text{m}$ ) and provide images representing temperature values per pixel. Thus, conventional, time-consuming ground-based gs measurements can be feasibly replaced by thermal images evaluating plant physiological status at different scales in short periods of time <sup>[10][11]</sup>. Additionally, highly sensitive thermal cameras with a relatively simple operational procedure have become more available to research groups, at a lower cost and at higher spatial resolution <sup>[12][13]</sup>. Moreover, TIR imaging is a very valuable method of stress detection prior to the appearance of symptoms since it operates out of the visual range of the spectrum <sup>[14]</sup>. However, some considerations must be taken when interpreting thermograms in terms of gs since plant surface temperature is mainly driven by environmental factors such as air temperature and relative humidity.

Despite the wide use of thermography applied to agronomy, this technique per se has a very limited capacity for diagnosis. Indeed, temperature raises may be due to stomatal closure, which is on its own an unspecific mechanism of plant defense against both abiotic and biotic stressors. Even more, temperature raises can also respond to a decreased capacity for water evaporation or even to the loss of vegetation <sup>[10]</sup>. In contrast, some stresses can cause temporary decreases in leaf temperature. That would be the case of some pathogens that can interfere in the regulation of stomatal movements to favor their entry to the mesophyll <sup>[15]</sup>. As a consequence, alterations in TIR parameters stand as ambiguous clues for diagnosis. Moreover, abiotic stress factors (mostly drought, soil salinity or extreme ambient temperature) also cause increases in canopy temperature. This is most important under natural conditions, where abiotic stressors are difficult to assess and avoid. Keeping in mind that under such conditions, several stress factors often affect the vegetation simultaneously, possible misinterpretations of TIR data would lead to inaccurate determination of the incidence and severity of a particular pathogen infection or even to a wrong diagnosis.

To overcome the restraints of thermography as a diagnostic technique, authors have increasingly applied it in combination with other imaging techniques. Roitsch et al. [16] and Sperschneider [17] reviewed the implementation of TIR cameras with other sensors, such as RGB, multi- or hyperspectral cameras, in phenotyping platforms. The identification of spatial and temporal patterns of TIR parameters in combination with other relevant vegetation indices (VIs) could be of great help to establish robust methods for the early diagnosis in crop fields. However, a preliminary analysis of a given plant-stressor interaction is desirable to obtain a stress-specific signature [18].

The use of complementary imaging techniques provides valuable and very complex information. This complexity is caused by the increasing number of dimensions that can be considered and the incessant improvements in their spatial and temporal resolution. To enhance our capacity for data analysis, most recent works have included data-mining in their analysis. This multidisciplinary approach, based on probability theory, statistics, decision theory, visualization and optimization, outperforms more conventional statistical analysis in terms of finding patterns in data [19][20]. Classifiers are algorithms able to learn patterns from a database of known samples and, based on that knowledge, to identify or categorize new samples [21]. When applied to agriculture, this approach facilitates the interpretation of data and the decision-making process to such an extent that no study appears to be complete without this type of analysis.

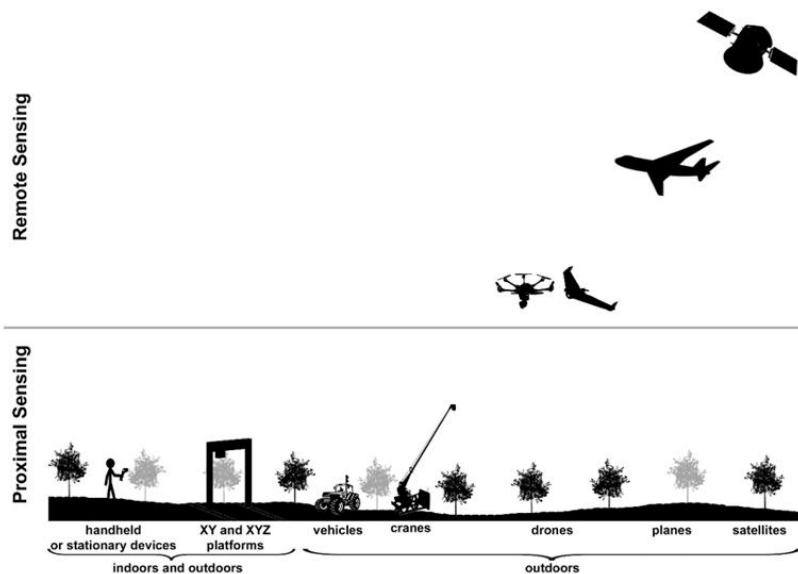


**Figure 1.** The most common platforms implementing thermal cameras at proximal and remote sensing scale.

Thermography is extensively used for stress detection from lab to field scale by either proximal or remote sensing (Figure 1). On one hand, proximal sensing (mainly in growth chambers and greenhouses) refers to imaging single leaves or entire plants from a close distance to the target. The camera could be mounted on a static stand or small and medium-size robots, including high-throughput platforms. On the other hand, remote sensing refers to measurements taken in open fields with imaging sensors implemented on a wide range of devices, such as cranes, vehicles, robots and unmanned aerial vehicles (UAVs; in which the image resolution depends on the flight height) to cover whole crop fields. Even larger areas (district to region scales) can be tackled thanks to the sensors onboard satellites (i. e. ASTER, Sentinel-3, ECOSTREES, or Landsat-7 and 8, among others). These sensors differ in their spatial resolution and also on the time resolution, depending on the revisiting frequency of the satellite over the particular area.

Physical and technical aspects of thermography, such as scientific principles applied to measurements and data correction methods [22][23][24][25], as well as practical considerations affecting thermal imagery for plant phenotyping [26][27], have been recently reviewed. Other aspects related to thermography, such as available imaging sensors and evaluation of their potential [28][29], their use in phenotyping platforms [16][30][31] or UAVs [24][32][33][34], and their applications have also deserved special attention by many authors. Moreover, other TIR applications have also been thoroughly reviewed elsewhere [18][22]. Furthermore, very recent works reviewed the state of the art in the application of artificial intelligence to stress detection [17][20]. Despite the vast number of works addressing the use of thermography for plant stress detection, little attention has been paid to the physiological perspective of temperature alterations related to stressed plants. Attending to this need, Pineda et al [35] revised the most relevant applications of thermography to agriculture with the main aim of providing TIR camera users with a collection of host plant–pathogen systems described in the literature in terms of thermal response and the mechanisms of plant defense involved.

## 2. Thermography Applied to Biotic Stress Detection at Proximal Sensing Scale

Stomata are the main natural entry of pathogens into the plant tissues. Hence, the regulation of the stomatal movements plays a key role in plant defense against microbes [36]. The recognition of a potential pathogen by plants usually triggers stomatal closure; to counteract this defense response, some pathogens are able to override the plant signaling pathways to activate stomatal aperture [37]. Other effects of pathogen infection include disturbances on leaf development, cell wall and leaf cuticle composition or integrity, alterations in the plant metabolism or even necrosis of the tissues. These physical and chemical disturbances affect the plant water status, which can be monitored by thermography [38][39][40].

### 2.1. Viral Infections

Even when some virosis cause alterations neither in  $g_s$  nor in leaf temperature [41], thermography is very often helpful in tracking viral infections on plants. Most of those works report temperature increases between +0.5 and +1.5 K; on the contrary, some works reported decreases in leaf temperature of -0.5 K relative to mock-controls. Hypersensitive response (HR) to Tobacco mosaic virus (TMV) could be visualized as spots of elevated temperature before any disease symptoms became visible on tobacco leaves. Those spots were confined to the site of infection as a result of the HR triggered by salicylic acid. On the other hand, no thermal response was observed on susceptible tobacco-TMV-infected plants [42]. In the case of Pepper middle mottle virus (PMMoV)-*Nicotiana benthamiana* plants, virus spreading through asymptomatic leaves could be first detected by an increase in temperature on the tissues around the main veins. This effect extended to adjacent tissues before the spreading of the virus across the midrib of the leaf, as shown by immunolocalization. Interestingly, the thermal symptoms caused by the most severe strain of PMMoV were detected before those caused by the less virulent one [43]. Among other tobamoviruses, Cucumber mosaic virus (CMV) and Cucumber green mottle mosaic virus (CGMMV) have a particular impact on cucumber production. Plants infected with CMV displayed homogeneously higher temperature in the whole inoculated leaf relative to the controls, whereas leaves of CGMMV-infected cucumber plants showed a heterogeneous temperature pattern, consisting of cold spots at the infection sites. However, none of those changes was detectable presymptomatically. Nevertheless, classificatory algorithms could early detect the infection caused by each pathogen when combining data obtained by TIR, fluorescence and hyperspectral imaging [44]. Another virus of agricultural interest is the Sweet potato feathery mottle virus, which is the most widespread virus that infects sweet potato plants, causing devastating problems when co-infecting with Sweet potato chlorotic stunt virus. Higher leaf temperatures were associated with more severe symptoms; thus, plants co-infected with both viruses displayed higher temperatures than single virus-infected plants [45].

### 2.2. Bacterial Infections

In the case of bacterial-infected plants, literature reports temperature changes relative to the controls ranging between -3.3 K and +3 K. The tumor caused by *Agrobacterium tumefaciens* in the hypocotyl of castor oil plant produces irreversible disruption of the plant epidermis and hence, the tumor lacks a protective cuticle against water loss. Moreover, stomata located at the tumor edge are hypertrophied and non-functional; as a consequence, the tumor surface was the coldest part of the plant [46]. Some works have studied the role of plant defense elicitors produced by bacterial pathogens. That is the case of the proteinaceous harpin synthesized by the bacterium *Erwinia amylovora*. When infiltrated in the leaves of *Nicotiana glauca* wild plants, harpin induced a marked presymptomatic cooling at the inoculation sites, followed by an increase of temperature during the HR [47]. The same trend was described for spots of bacterial canker caused by *Pseudomonas syringae* pv. *actinidiae* on kiwifruit leaves [48]. The decrease in temperature localized at the infection sites could be related to bacterial virulence factors that actively open the stomata by interfering with hormonal signaling pathways leading to stomatal closure [49]. On the other hand, it is well known that recognition of some pathogen-associated molecular patterns triggers stomatal closure to impede bacterial entrance through these natural apertures [15]. In bean plants, *P. syringae* pv. *tomato* DC3000 induces an HR, whereas *P. syringae* pv. *phaseolicola* 1448A produces systemic infection. First symptoms are evident after 10 h and 2 days post-infection, respectively. Thermography could presymptomatically reveal those bacterial challenges as an increase of temperature of the inoculated areas at 1 and 2 h post-infection in the case of HR and systemic infection, respectively [50].

Several works have addressed the effect of the *Dickeya dadantii* infection on plant transpiration by thermography. This bacterium usually produces soft-rot, a characteristic tissue maceration, as in the case of *N. benthamiana* infected at high inoculum dose. After mechanical infiltration, the temperature of the affected areas raised presymptomatically, linked to an increase in hormones controlling stomatal closure. In subsequent days, the temperature continued rising, affecting the whole leaf. However, *N. benthamiana* can activate an efficient defense response against *D. dadantii* when the plant is inoculated at doses resembling the natural infection. In this case, after an initial increase in temperature of the infiltrated area, infected plants could recover, and temperature subsequently decreased [51]. Independently of the inoculum dose, *D.*

*D. dadantii* does not cause tissue maceration on melon leaves. It produces brownish spots at the inoculation sites that evolve chlorosis in the surrounding tissues in successive days; those symptoms appeared earlier when high dose concentrations were applied. Only infiltrated areas shown increased temperatures at the beginning of the infection process when inoculated at a low dose; the whole leaf finally displaying higher temperature respecting to the controls. However, when a high inoculum dose was applied, the whole melon leaf displayed a higher temperature [52]. The whole leaf of another cucurbit, such as zucchini, displayed higher temperature relative to the controls when inoculated with *D. dadantii*, whereas visual symptoms (different degrees of chlorosis proportional to the inoculated dose) were circumscribed to the infiltrated spots [53][54]. Features extracted from TIR and multicolor fluorescence images were used to feed algorithms, which provided a good performance of classification of plants into categories of infected and controls in both melon and zucchini plants [52][53].

### 2.3. Interactions with Pathogenic Fungi and Oomycetes

Thermography has been widely used to assess the effect of fungi and oomycetes on host plant transpiration. Depending on how these pathogens interact with host plants, initial phases of pathogenesis can induce increases or decreases in leaf temperatures affecting only the inoculation sites or whole leaves. Subsequent symptoms development may cause transitory drops in temperature as the affected cells die and lose water. Later infection phases usually lead to an increase in temperature due to the lack of natural cooling of the necrotic tissues. Concerning healthy areas, it is possible to find in the cited literature that biotrophic fungi and oomycetes can cause temperature decreases ranging from  $-0.1$  to  $-2.5$  K, whereas increases have been registered from  $+0.6$  to  $+2$  K. For their part, hemibiotrophic pathogens can decrease leaf temperature between  $-0.6$  and  $-2.2$  K, or contrary, increase it in  $+0.4$  to  $+7.5$  K. Finally, it is possible to register temperatures decreases between  $-2$  and  $-5$  K and increases ranging from  $+0.3$  to  $+9$  K when necrotrophic fungi are studied by TIR imaging.

Concerning infections caused by biotrophic fungi leaves from wheat plants infected with *Blumeria graminis* or *Puccinia striiformis* (fungi causing powdery mildew and stripe rust, respectively) displayed low temperatures due to the very low resistance to water evaporation of growing mycelia [55][56]. The phytopathogens *Pseudoperonospora cubensis* and *Podosphaera xanthii* are the causal agents of cucumber downy mildew and cucurbits powdery mildew, respectively. In cucumber leaves, these pathogens produce infective spots with lower temperatures than the surrounding healthy areas due to an abnormal stomatal opening. In the case of *P. xanthii* infection, the thermographic detection was not presymptomatic, whereas disease caused by *P. cubensis* could be revealed one day before the appearance of symptoms. Under laboratory conditions, the MTD increased during both pathogenesis and was related to disease severity [44][57][59][58]. Despite being a biotrophic oomycete, *P. cubensis* also produces necrosis in the latest infection phase associated with an increase in cucumber leaf temperature [57][59]. Leaves of rose infected with the fungus *Podosphaera pannosa* var. *rosae* (causal agent of powdery mildew in roses) showed a presymptomatic decrease in temperature. Furthermore, two algorithms were trained on features extracted from TIR images, obtaining high accuracy in classifying healthy and infected plants [60]. Raza et al. [61] also used information extracted from TIR and RGB pictures to automatically detect tomato plants infected with *Oidium neolycopersici* in a presymptomatic way, but the work did not address the physiological changes caused by the fungus.

Regarding hemibiotrophic fungi, TIR imaging could describe the severity of the infection, which could be related to the disease stages but also to the host plant resistance to the pathogen. Thus, Oerke et al. [62] and Belin et al. [63] analyzed apple trees suffering from apple scab. In that case, the detection of infection, as well as differences in the virulence of several *Venturia inaequalis* isolates infecting apple trees, were detected more accurately by thermography than by chlorophyll fluorescence imaging. The thermal response was presymptomatic and consisted of spots of decreased temperature due to the subcuticular growth of *V. inaequalis*. A soilborne fungus, *Rhizoctonia solani*, induces necrosis in lettuce plants, which could be visualized as an increase in leaf temperature and MTD [64]. The damage produced by another soilborne fungus, *Fusarium oxysporum*, to whole cucumber leaves could be detected as a presymptomatic raise in temperature induced by abscisic acid, followed by a slight decrease as wilt symptoms developed. Finally, the temperature of whole leaves presenting necrosis increased again [65]. On the contrary, pea plants infected with this fungus showed an early and slight reduction of temperature compared to the control plants. At an advanced stage of the infection, the leaf temperature increased above control levels in the case of susceptible plants, whereas the temperature of those showing *F. oxysporum*-resistance remained similar to the controls [66].

In the case of infections caused by necrotrophic fungi, sugar beet plants inoculated with *Cercospora beticola* (causal agent of *Cercospora* leaf spot) displayed spots of presymptomatic low temperature corresponding to the infection sites. Cold spots appeared progressively until covering the whole leaf surface, whereas lesions were hardly visible by the naked eye. Toxins influencing cell membrane permeability and produced by *C. beticola* could account for this temperature decrease [42]. *Aspergillus carbonarius* is a fungus causing sour rot of grape berries and produces ochratoxin-As, toxic for

humans. Mycelium growth areas showed low temperatures that identified affected fruit sites at the very early stages of *A. carbonarius* infection [67]. Thermography also revealed that *Alternaria alternata*, *A. brassicae* and *A. brassicicola* caused a decrease of temperature during the first seven days of infection on oilseed rape leaves, followed by a temperature increase in successive days. However, those plants inoculated with *A. dauci* only developed increases of mean temperature at 21 days after inoculation [68]. The infection with *Botrytis cinerea* (gray mold) on bean plants caused a presymptomatic increase of temperature at the infection sites. In subsequent days, leaves developed hot brownish necrotic lesions surrounded by a lower temperature area [69]. On the contrary, *B. cinerea*-infected roses first showed a decrease of temperature at regions where lesions were initially formed, followed by a rise in temperature once necrosis occurred [60]. *Rosellinia necatrix* (soilborne fungus causing white root rot) is one of the most important constraints to production for a wide range of woody crops such as avocado. In the late phases of *R. necatrix* infection, trees undergo a water deficit in the aerial part due to failure of the root system [70]. As a result, infected plants experienced a significant increase in leaf temperature from the early symptomatic stage onwards [71]. Furthermore, infected avocado trees in an orchard could be detected by thermography (see Section 3) [72].

## 2.4. Herbivory and Parasitic Plants

Herbivore insects disrupt the integrity of leaves, leading to uncontrolled water loss from wounds and triggering intricate processes that affect gas exchange also in the remaining leaf tissue. Thus, it is possible to find temperature drops from  $-0.3$  to  $-3$  K in the literature. TIR images of soybean leaflets affected by corn earworm caterpillars (*Helicoverpa zea*) showed that leaf areas adjacent to wounds were cooler than distant regions or sister leaflets [73]. The same leaf temperature pattern was visible after injuries caused by cabbage looper (*Trichoplusia ni*) instars on *Arabidopsis* [74], tobacco hornworm (*Manduca sexta*) on *Nicotiana attenuata* [75], or larval gypsy moth (*Lymantria dispar*) and gall damage produced by midge flies (*Harmandia* sp.) on aspen leaves [76]. When elevated CO<sub>2</sub> was applied to the atmosphere, the cooling effect of gall formation on remaining leaf tissue was reduced [76].

Thermography was also useful in the detection of plants infested by parasites, revealing temperature increases (from  $+0.4$  to  $+0.9$  K) due to a reduction in the plant water uptake by affected roots. Examples of these interactions are the nematode *Heterodera schachtii* with susceptible sugar beet cultivars [77], as well as the obligatory root parasitic plant *Orobanche cumana* (broomrape) and sunflower [78]. The early detection of broomrape by nondestructive techniques was unprecedented since natural infestation causes subtle alterations on host physiology and proceeds unnoticed until the emergence of the floral shoots, by the time of sunflower bloom.

## 3. Thermography Applied to Biotic Stress Detection at Remote Sensing Scale

In crop fields, thermography has facilitated the detailed analysis of crop fields affected by pathogens, helping in the localization of areas where plants are affected and requiring urgent intervention [79]. In general, pathogen infected plants show changes their temperature of  $-2$  K to  $+3.1$  K, relative to the temperature of healthy plants; however, it is worth noticing that these values should be handled with care depending on the sensitivity and the accuracy of the used TIR cameras. The identification of potentially infected plants using classifiers provides accuracies ranging between 59-89%, depending on the applied algorithm and parameters used to feed it.

In a susceptible cultivar of sugar beet, canopy temperature correlated significantly with the density of the nematode parasite *H. schachtii* [80]. Kiwifruit trees infected by *P. syringae* pv. *actinidiae* were significantly warmer than the healthy ones, being localized in the outer canes of the canopy [48]. Temperature increases measured on *Dothistroma septosporum*-infected pines (causal agent of red band needle blight) and on *Zymoseptoria tritici*-infected winter wheat (causing septoria leaf blotch) could be positively correlated to the damages caused by these hemi-biotrophic fungi [40][81]. Necrotic spots on leaves from woody trees caused by three fungi (*Mycosphaerella cerasella*, *Elsinoe corni* and *Tubakia dryina*) could also be detected as dots with higher temperatures relative to healthy areas [82].

The fusion of thermography with other imaging techniques such as multi- or hyper-spectral reflectance or chlorophyll fluorescence imaging cameras is very often a more adequate approach for stress detection. The combination with chlorophyll fluorescence imaging allowed monitoring several constraints (fungal infection, galls and chewing damages caused by arthropods) in understory hardwood saplings. Thus, changes in transpiration could be related to photosynthesis impairment in affected trees [83]. However, the combination of TIR imaging with multi- or hyper-spectroscopy reflectance is more feasible since both techniques are based on passive measurements. Moreover, it is possible to obtain multiple reflectance VIs that could correlate with physiological parameters. Furthermore, VIs, together with temperature derived parameters, could be implemented on algorithms, to classify plants into categories of interest in

the earliest stages of infection. That was the case of important bacterial diseases causing high impact on both agriculture and environment, such as citrus greening or Huanglongbing in citrus trees [84], or *Xylella fastidiosa*, a quarantine pathogen, in olive orchards [85].

In the case of diseases caused by foliar fungal pathogens, the joint use of thermography and reflectance made possible to discriminate between severity levels. That was the case of red leaf blotch (caused by *Polystigma amygdalinum*) in almond trees [86] and also early and late leaf spot diseases (caused by *Passalora arachidicola* S. Hori and *Cercosporidium personatum*, respectively) on peanut trees [87].  $\Delta T$  correlated with disease severity caused by soil-borne fungal pathogens, such as *Verticillium dahliae* (causal agent of Verticillium wilt) in olive trees or *R. necatrix* in avocado trees. Moreover, classifying algorithms applied to the data obtained by spectral and TIR imaging could identify affected trees with high accuracy [72][88][89]. Minimum temperature corrected by air temperature could also be a good indicator of stress. This parameter showed a negative correlation with the normalized difference vegetation index (NDVI) in opium poppy orchards infected by the oomycete *Peronospora arborescens* (causal agent of downy mildew) [90]. Furthermore, a strong relationship between yield, several VIs and canopy temperature was observed in maize plants suffering tar spot complex (caused by *Phyllachora maydis* and *Monographella maydis*) [91], as well as in chickpea infected with *Ascochyta rabiei* (causing *Ascochyta* blight disease) [92].

---

## References

1. Stevanović, M.; Popp, A.; Lotze-Campen, H.; Dietrich, J.P.; Müller, C.; Borsch, M.; Schmitz, C.; Bodirsky, B.L.; Humpenöder, F.; Weindl, I. The impact of high-end climate change on agricultural welfare. *Science Advances* 2016, 2, e1501452; DOI:10.1126/sciadv.1501452.
2. Carvajal-Yepes, M.; Cardwell, K.; Nelson, A.; Garrett, K.A.; Giovani, B.; Saunders, D.G.O.; Kamoun, S.; Legg, J.P.; Verdier, V.; Lessel, J., et al. A global surveillance system for crop diseases. *Science* 2019, 364, 1237-1239; DOI:10.1126/science.aaw1572.
3. Zhan, J.; Thrall, P.H.; Papaix, J.; Xie, L.; Burdon, J.J. Playing on a Pathogen's Weakness: Using Evolution to Guide Sustainable Plant Disease Control Strategies. *Annu. Rev. Phytopathol.* 2015, 53, 19-43; DOI:10.1146/annurev-phyto-080614-120040.
4. Mahlein, A.-K. Plant disease detection by imaging sensors – Parallels and specific demands for precision agriculture and plant phenotyping. *Plant Dis.* 2016, 100, 241-251; DOI:10.1094/pdis-03-15-0340-fe.
5. Jones, H. *Plants and microclimate: a quantitative approach to environmental plant physiology*, Third Edition ed.; Cambridge University Press: United Kingdom, 2014; Vol. 56.
6. Prashar, A.; Yildiz, J.; McNicol, J.W.; Bryan, G.J.; Jones, H.G. Infra-red thermography for high throughput field phenotyping in *Solanum tuberosum*. *PLoS One* 2013, 8, e65816; DOI:10.1371/journal.pone.0065816.
7. Fuchs, M.; Tanner, C.B. Infrared thermometry of vegetation. *Agron. J.* 1966, 58, 597-601.
8. Milthorpe, F.L.; Spencer, E.J. Experimental studies of the factors controlling transpiration. *J. Exp. Bot.* 1957, 8, 413-437; DOI:10.1093/jxb/8.3.413.
9. Scarth, G.W.; Loewy, A.; Shaw, M. Use of the infrared total absorption method for estimating the time course of photosynthesis and transpiration. *Canadian Journal of Research* 1948, 26c, 94-107; DOI:10.1139/cjr48c-010.
10. Jones, H.G. Use of thermography for quantitative studies of spatial and temporal variation of stomatal conductance over leaf surfaces. *Plant, Cell and Environment* 1999, 22, 1043-1055; DOI:10.1046/j.1365-3040.1999.00468.x.
11. Jones, H.G. Application of thermal imaging and infrared sensing in plant physiology and ecophysiology. In *Adv. Bot. Res.*, Academic Press: 2004; Vol. 41, pp. 107-163.
12. Ishimwe, R.; Abutaleb, K.; Ahmed, F. Applications of thermal imaging in agriculture - A review. *Advances in Remote Sensing* 2014, 3, 13; DOI:10.4236/ars.2014.33011.
13. Khanal, S.; Fulton, J.; Shearer, S. An overview of current and potential applications of thermal remote sensing in precision agriculture. *Comput. Electron. Agric.* 2017, 139, 22-32; DOI:10.1016/j.compag.2017.05.001.
14. Chaerle, L.; Van der Straeten, D. Seeing is believing: imaging techniques to monitor plant health. *Biochim. Biophys. Acta* 2001, 1519, 153-166.
15. Zeng, W.; Melotto, M.; He, S.Y. Plant stomata: a checkpoint of host immunity and pathogen virulence. *Curr. Opin. Biotechnol.* 2010, 21, 599-603; DOI:10.1016/j.copbio.2010.05.006.
16. Roitsch, T.; Cabrera-Bosquet, L.; Fournier, A.; Ghamkhar, K.; Jiménez-Berni, J.A.; Pinto, F.; Ober, E.S. Review: New sensors and data-driven approaches—A path to next generation phenomics. *Plant Sci.* 2019, 282, 2-10; DOI:10.1016/j.pl

17. Sperschneider, J. Machine learning in plant–pathogen interactions: empowering biological predictions from field scale to genome scale. *New Phytol.* 2019, 10.1111/nph.15771; DOI:10.1111/nph.15771.
18. Saglam, A.; Chaerle, L.; Van Der Straeten, D.; Valcke, R. Promising monitoring techniques for plant science: Thermal and chlorophyll fluorescence imaging. In *Photosynthesis, Productivity and Environmental Stress*, 2019; 10.1002/9781119501800.ch12pp. 241-266.
19. Singh, A.; Ganapathysubramanian, B.; Singh, A.K.; Sarkar, S. Machine learning for high-throughput stress phenotyping in plants. *Trends Plant Sci.* 2016, 21, 110-124; DOI:10.1016/j.tplants.2015.10.015.
20. Gao, Z.; Luo, Z.; Zhang, W.; Lv, Z.; Xu, Y. Deep learning application in plant stress imaging: A review. *AgriEngineering* 2020, 2, 430-446; DOI:10.3390/agriengineering2030029.
21. Liakos, K.G.; Busato, P.; Moshou, D.; Pearson, S.; Bochtis, D. Machine learning in agriculture: A review. *Sensors (Basel)* 2018, 18, 2674; DOI:10.3390/s18082674.
22. Still, C.; Powell, R.; Aubrecht, D.; Kim, Y.; Helliker, B.; Roberts, D.; Richardson, A.D.; Goulden, M. Thermal imaging in plant and ecosystem ecology: applications and challenges. *Ecosphere* 2019, 10, e02768; DOI:10.1002/ecs2.2768.
23. Jones, H.G. Thermal imaging and infrared sensing in plant ecophysiology. In *Advances in Plant Ecophysiology Techniques*, Springer: 2018; 10.1016/S0065-2296(04)41003-9pp. 135-151.
24. Messina, G.; Modica, G. Applications of UAV thermal imagery in precision agriculture: State of the art and future research outlook. *Remote Sens.* 2020, 12, 1491; DOI:10.3390/rs12091491.
25. Violet-Chabrand, S.; Lawson, T. Dynamic leaf energy balance: deriving stomatal conductance from thermal imaging in a dynamic environment. *J. Exp. Bot.* 2019, 70, 2839-2855; DOI:10.1093/jxb/erz068.
26. Kelly, J.; Kljun, N.; Olsson, P.-O.; Mihai, L.; Liljeblad, B.; Weslien, P.; Klemedtsson, L.; Eklundh, L. Challenges and best practices for deriving temperature data from an uncalibrated UAV thermal infrared camera. *Remote Sens.* 2019, 11, 567; DOI:10.3390/rs11050567.
27. Prashar, A.; Jones, H.G. Infra-red thermography as a high-throughput tool for field phenotyping. *Agronomy* 2014, 4, 397-417.
28. Sagan, V.; Maimaitijiang, M.; Sidike, P.; Eblimit, K.; Peterson, K.T.; Hartling, S.; Esposito, F.; Khanal, K.; Newcomb, M.; Pauli, D. UAV-based high resolution thermal imaging for vegetation monitoring, and plant phenotyping using ICI 8640 P, FLIR Vue Pro R 640, and thermoMap cameras. *Remote Sens.* 2019, 11, 330; DOI:10.3390/rs11030330.
29. Zhang, J.; Huang, Y.; Pu, R.; Gonzalez-Moreno, P.; Yuan, L.; Wu, K.; Huang, W. Monitoring plant diseases and pests through remote sensing technology: A review. *Comput. Electron. Agric.* 2019, 165, 104943; DOI:10.1016/j.compag.2019.104943.
30. Li, Z.; Guo, R.; Li, M.; Chen, Y.; Li, G. A review of computer vision technologies for plant phenotyping. *Comput. Electron. Agric.* 2020, 176, 105672; DOI:10.1016/j.compag.2020.105672.
31. Costa, J.M.; Marques da Silva, J.; Pinheiro, C.; Barón, M.; Mylona, P.; Centritto, M.; Haworth, M.; Loreto, F.; Uzilday, B.; Turkan, I., et al. Opportunities and limitations of crop phenotyping in southern European countries. *Front. Plant Sci.* 2019, 10, 1125; DOI:10.3389/fpls.2019.01125.
32. Barbedo, J.G.A. A review on the use of unmanned aerial vehicles and imaging sensors for monitoring and assessing plant stresses. *Drones* 2019, 3, 40; DOI:10.3390/drones3020040.
33. Maes, W.H.; Steppe, K. Perspectives for remote sensing with unmanned aerial vehicles in precision agriculture. *Trends Plant Sci.* 2019, 24, 152-164; DOI:10.1016/j.tplants.2018.11.007.
34. Zhang, C.; Valente, J.; Kooistra, L.; Guo, L.; Wang, W. Opportunities of UAVs in orchard management. *Int. Arch. Photogramm. Remote Sens. Spatial Inf. Sci.* 2019, XLII-2/W13, 673-680; DOI:10.5194/isprs-archives-XLII-2-W13-673-2019.
35. Pineda, M.; Barón, M.; Pérez-Bueno, M.-L. Thermal imaging for plant stress detection and phenotyping. *Remote Sens.* 2021, 13, 68; DOI:10.3390/rs13010068.
36. Sawinski, K.; Mersmann, S.; Robotzek, S.; Bohmer, M. Guarding the green: pathways to stomatal immunity. *Mol. Plant Microbe Interact.* 2013, 26, 626-632; DOI:10.1094/MPMI-12-12-0288-CR.
37. Agurla, S.; Raghavendra, A.S. Convergence and divergence of signaling events in guard cells during stomatal closure by plant hormones or microbial elicitors. *Front. Plant Sci.* 2016, 7, 1332; DOI:10.3389/fpls.2016.01332.
38. Barón, M.; Pineda, M.; Pérez-Bueno, M.L. Picturing pathogen infection in plants. *Z. Naturforsch. C Bio. Sci.* 2016, 71, 355-368; DOI:10.1515/znc-2016-0134.

39. Grimmer, M.K.; John Foulkes, M.; Paveley, N.D. Foliar pathogenesis and plant water relations: a review. *J. Exp. Bot.* 2012, 63, 4321-4331; DOI:10.1093/jxb/ers143.
40. Smigaj, M.; Gaulton, R.; Suárez, J.C.; Barr, S.L. Canopy temperature from an Unmanned Aerial Vehicle as an indicator of tree stress associated with red band needle blight severity. *Forest Ecol. Manag.* 2019, 433, 699-708; DOI:10.1016/j.foreco.2018.11.032.
41. Montero, R.; Pérez-Bueno, M.L.; Barón, M.; Florez-Sarasa, I.; Tohge, T.; Fernie, A.R.; El Aou Ouad, H.; Flexas, J.; Bota, J. Alterations in primary and secondary metabolism in *Vitis vinifera* 'Malvasía de Banyalbufar' upon infection with Grapevine leafroll associated virus 3 (GLRaV-3). *Physiol. Plant.* 2016, 157, 442-452; DOI:10.1111/ppl.12440.
42. Chaerle, L.; Hagenbeek, D.; De Bruyne, E.; Valcke, R.; Van der Straeten, D. Thermal and chlorophyll-fluorescence imaging distinguish plant-pathogen interactions at an early stage. *Plant Cell Physiol.* 2004, 45, 887-896; DOI:10.1093/pcp/pch097.
43. Chaerle, L.; Pineda, M.; Romero-Aranda, R.; Van der Straeten, D.; Barón, M. Robotized thermal and chlorophyll fluorescence imaging of Pepper mild mottle virus infection in *Nicotiana benthamiana*. *Plant Cell Physiol.* 2006, 47, 1323-1336; DOI:10.1093/pcp/pcj102.
44. Berdugo, C.A.; Zito, R.; Paulus, S.; Mahlein, A.K. Fusion of sensor data for the detection and differentiation of plant diseases in cucumber. *Plant Pathol.* 2014, 63, 1344-1356; DOI:10.1111/ppa.12219.
45. Wang, L.; Poque, S.; Valkonen, J.P. Phenotyping viral infection in sweetpotato using a high-throughput chlorophyll fluorescence and thermal imaging platform. *Plant Methods* 2019, 15, 116; DOI:10.1186/s13007-019-0501-1.
46. Schurr, U.; Schuberth, B.; Aloni, R.; Pradel, K.S.; Schmundt, D.; Jahne, B.; Ullrich, C.I. Structural and functional evidence for xylem-mediated water transport and high transpiration in *Agrobacterium tumefaciens*-induced tumors of *Ricinus communis*. *Botanica Acta* 1996, 109, 405-411; DOI:10.1111/j.1438-8677.1996.tb00590.x.
47. Boccara, M.; Boue, C.; Garmier, M.; De Paepe, R.; Boccara, A.C. Infra-red thermography revealed a role for mitochondria in pre-symptomatic cooling during harpin-induced hypersensitive response. *Plant J.* 2001, 28, 663-670; DOI:10.1046/j.1365-3113x.2001.01186.x.
48. Maes, W.H.; Minchin, P.E.H.; Snelgar, W.P.; Steppe, K. Early detection of *Psa* infection in kiwifruit by means of infrared thermography at leaf and orchard scale. *Funct. Plant Biol.* 2014, 41, 1207-1220; DOI:10.1071/fp14021.
49. Zheng, X.Y.; Spivey, N.W.; Zeng, W.; Liu, P.P.; Fu, Z.Q.; Klessig, D.F.; He, S.Y.; Dong, X. Coronatine promotes *Pseudomonas syringae* virulence in plants by activating a signaling cascade that inhibits salicylic acid accumulation. *Cell Host and Microbe* 2012, 11, 587-596; DOI:10.1016/j.chom.2012.04.014.
50. Pérez-Bueno, M.L.; Pineda, M.; Díaz-Casado, E.; Barón, M. Spatial and temporal dynamics of primary and secondary metabolism in *Phaseolus vulgaris* challenged by *Pseudomonas syringae*. *Physiol. Plant.* 2015, 153, 161-174; DOI:10.1111/ppl.12237.
51. Pérez-Bueno, M.L.; Granum, E.; Pineda, M.; Flors, V.; Rodríguez-Palenzuela, P.; López-Solanilla, E.; Barón, M. Temporal and spatial resolution of activated plant defense responses in leaves of *Nicotiana benthamiana* infected with *Dickeya dadantii*. *Front. Plant Sci.* 2016, 6, 1209; DOI:10.3389/fpls.2015.01209.
52. Pineda, M.; Pérez-Bueno, M.L.; Barón, M. Detection of bacterial infection in melon plants by classification methods based on imaging data. *Front. Plant Sci.* 2018, 9, 164; DOI:10.3389/fpls.2018.00164.
53. Pérez-Bueno, M.L.; Pineda, M.; Cabeza, F.; Barón Ayala, M. Multicolor fluorescence imaging as a candidate for disease detection in plant phenotyping. *Front. Plant Sci.* 2016, 7, 1790; DOI:10.3389/fpls.2016.01790.
54. Pineda, M.; Luisa Perez-Bueno, M.; Paredes, V.; Barón, M. Use of multicolour fluorescence imaging for diagnosis of bacterial and fungal infection on zucchini by implementing machine learning. *Funct. Plant Biol.* 2017, 44, 563-572; DOI:10.1071/FP16164.
55. Hellebrand, H.J.; Herppich, W.B.; Beuche, H.; Dammer, K.-H.; Linke, M.; Flath, K. Investigations of plant infections by thermal vision and NIR imaging. *International Agrophysics* 2006, 20, 1-10.
56. Yao, Z.; He, D.; Lei, Y. Thermal imaging for early nondestructive detection of wheat stripe rust. In *Proceedings of 2018 ASABE Annual International Meeting*; p. 1.
57. Lindenthal, M.; Steiner, U.; Dehne, H.W.; Oerke, E.C. Effect of downy mildew development on transpiration of cucumber leaves visualized by digital infrared thermography. *Phytopathology* 2005, 95, 233-240; DOI:10.1094/PHYTO-95-0233.
58. Wen, D.-M.; Chen, M.-X.; Zhao, L.; Ji, T.; Li, M.; Yang, X.-T. Use of thermal imaging and Fourier transform infrared spectroscopy for the pre-symptomatic detection of cucumber downy mildew. *Eur. J. Plant Pathol.* 2019, 155, 405-416; DOI:10.1007/s10658-019-01775-2.

59. Oerke, E.C.; Steiner, U.; Dehne, H.W.; Lindenthal, M. Thermal imaging of cucumber leaves affected by downy mildew and environmental conditions. *J. Exp. Bot.* 2006, 57, 2121-2132; DOI:10.1093/jxb/erj170.
60. Jafari, M.; Minaei, S.; Safaie, N. Detection of pre-symptomatic rose powdery-mildew and gray-mold diseases based on thermal vision. *Infrared Physics and Technology* 2017, 85, 170-183; DOI:10.1016/j.infrared.2017.04.023.
61. Raza, S.; Prince, G.; Clarkson, J.P.; Rajpoot, N.M. Automatic detection of diseased tomato plants using thermal and stereo visible light images. *PLoS One* 2015, 10, e0123262; DOI:10.1371/journal.pone.0123262.
62. Oerke, E.C.; Fröhling, P.; Steiner, U. Thermographic assessment of scab disease on apple leaves. *Precis. Agric.* 2011, 12, 699-715; DOI:10.1007/s11119-010-9212-3.
63. Belin, É.; Rousseau, D.; Boureau, T.; Caffier, V. Thermography versus chlorophyll fluorescence imaging for detection and quantification of apple scab. *Comput. Electron. Agric.* 2013, 90, 159-163; DOI:10.1016/j.compag.2012.09.014.
64. Sandmann, M.; Grosch, R.; Graefe, J. The use of features from fluorescence, thermography, and NDVI imaging to detect biotic stress in lettuce. *Plant Dis.* 2018, 102, 1101-1107; DOI:10.1094/PDIS-10-17-1536-RE.
65. Wang, M.; Ling, N.; Dong, X.; Zhu, Y.; Shen, Q.; Guo, S. Thermographic visualization of leaf response in cucumber plants infected with the soil-borne pathogen *Fusarium oxysporum* f. sp. *cucumerinum*. *Plant Physiol. Biochem.* 2012, 61, 153-161; DOI:10.1016/j.plaphy.2012.09.015.
66. Rispaill, N.; Rubiales, D. Rapid and efficient estimation of pea resistance to the soil-borne pathogen *Fusarium oxysporum* by infrared imaging. *Sensors (Basel)* 2015, 15, 3988-4000; DOI:10.3390/s150203988.
67. Mastrodimos, N.; Lentzou, D.; Templalexis, C.; Tsitsigiannis, D.I.; Xanthopoulos, G. Development of thermography methodology for early diagnosis of fungal infection in table grapes: The case of *Aspergillus carbonarius*. *Comput. Electron. Agric.* 2019, 165, 104972; DOI:10.1016/j.compag.2019.104972.
68. Baranowski, P.; Jedryczka, M.; Mazurek, W.; Babula-Skowronska, D.; Siedliska, A.; Kaczmarek, J. Hyperspectral and thermal imaging of oilseed rape (*Brassica napus*) response to fungal species of the genus *Alternaria*. *PLoS One* 2015, 10, e0122913; DOI:10.1371/journal.pone.0122913.
69. Chaerle, L.; Hagenbeek, D.; Vanrobaeys, X.; Van Der Straeten, D. Early detection of nutrient and biotic stress in *Phaseolus vulgaris*. *Int. J. Remote Sens.* 2007, 28, 3479-3492; DOI:10.1080/01431160601024259.
70. Ploetz, R.; Schaffer, B. Effects of flooding and *Phytophthora* root rot on net gas exchange and growth of avocado. *Phytopathology* 1989, 79, 204-208.
71. Granum, E.; Pérez-Bueno, M.L.; Calderón, C.E.; Ramos, C.; de Vicente, A.; Cazorla, F.M.; Barón, M. Metabolic responses of avocado plants to stress induced by *Rosellinia necatrix* analysed by fluorescence and thermal imaging. *Eur. J. Plant Pathol.* 2015, 142, 625-632; DOI:10.1007/s10658-015-0640-9.
72. Pérez-Bueno, M.L.; Pineda, M.; Vida, C.; Fernández-Ortuño, D.; Torés, J.A.; de Vicente, A.; Cazorla, F.M.; Barón, M. Detection of white root rot in avocado trees by remote sensing. *Plant Dis.* 2019, 103, 1119-1125; DOI:10.1094/PDIS-10-18-1778-RE.
73. Aldea, M.; Hamilton, J.G.; Resti, J.P.; Zangerl, A.R.; Berenbaum, M.R.; DeLucia, E.H. Indirect effects of insect herbivory on leaf gas exchange in soybean. *Plant Cell Environ.* 2005, 28, 402-411; DOI:10.1111/j.1365-3040.2005.01279.x.
74. Tang, J.Y.; Zielinski, R.E.; Zangerl, A.R.; Crofts, A.R.; Berenbaum, M.R.; DeLucia, E.H. The differential effects of herbivory by first and fourth instars of *Trichoplusia ni* (Lepidoptera: Noctuidae) on photosynthesis in *Arabidopsis thaliana*. *J. Exp. Bot.* 2006, 57, 527-536; DOI:10.1093/jxb/erj032.
75. Nabity, P.D.; Zavala, J.A.; DeLucia, E.H. Herbivore induction of jasmonic acid and chemical defences reduce photosynthesis in *Nicotiana attenuata*. *J. Exp. Bot.* 2013, 64, 685-694; DOI:10.1093/jxb/ers364.
76. Nabity, P.D.; Hillstrom, M.L.; Lindroth, R.L.; DeLucia, E.H. Elevated CO<sub>2</sub> interacts with herbivory to alter chlorophyll fluorescence and leaf temperature in *Betula papyrifera* and *Populus tremuloides*. *Oecologia* 2012, 169, 905-913; DOI:10.1007/s00442-012-2261-8.
77. Joalland, S.; Screpanti, C.; Liebisch, F.; Varella, H.V.; Gaume, A.; Walter, A. Comparison of visible imaging, thermography and spectrometry methods to evaluate the effect of *Heterodera schachtii* inoculation on sugar beets. *Plant Methods* 2017, 13, 14; DOI:10.1186/s13007-017-0223-1.
78. Ortiz-Bustos, C.M.; Pérez-Bueno, M.L.; Barón, M.; Molinero-Ruiz, L. Use of blue-green fluorescence and thermal imaging in the early detection of sunflower infection by the root parasitic weed *Orobanche cumana* Wallr. *Front. Plant Sci.* 2017, 8, 833; DOI:10.3389/fpls.2017.00833.
79. Sankaran, S.; Mishra, A.; Ehsani, R.; Davis, C. A review of advanced techniques for detecting plant diseases. *Comput. Electron. Agric.* 2010, 72, 1-13; DOI:10.1016/j.compag.2010.02.007.

80. Schmitz, A.; Kiewnick, S.; Schlang, J.; Sikora, R.A. Use of high resolution digital thermography to detect *Heterodera schachtii* infestation in sugar beets. *Communications in Agricultural and Applied Biological Sciences* 2004, 69, 359-363.
81. Wang, Y.; Zia-Khan, S.; Owusu-Adu, S.; Miedaner, T.; Müller, J. Early detection of *Zymoseptoria tritici* in winter wheat by infrared thermography. *Agriculture* 2019, 9, 139; DOI:10.3390/agriculture9070139.
82. Park, J.; Kim, K.W. Outdoor infrared imaging for spatial and temporal thermography: A case study of necrotic versus healthy leaf areas on woody plants. *J. Phytopathol.* 2020, 10.1111/jph.12959; DOI:10.1111/jph.12959.
83. Aldea, M.; Hamilton, J.G.; Resti, J.P.; Zangerl, A.R.; Berenbaum, M.R.; Frank, T.D.; Delucia, E.H. Comparison of photo synthetic damage from arthropod herbivory and pathogen infection in understory hardwood saplings. *Oecologia* 2006, 149, 221-232; DOI:10.1007/s00442-006-0444-x.
84. Sankaran, S.; Maja, J.M.; Buchanon, S.; Ehsani, R. Huanglongbing (citrus greening) detection using visible, near infrared and thermal imaging techniques. *Sensors* 2013, 13, 2117-2130; DOI:10.3390/s130202117.
85. Zarco-Tejada, P.J.; Camino, C.; Beck, P.S.A.; Calderon, R.; Hornero, A.; Hernández-Clemente, R.; Kattenborn, T.; Montes-Borrego, M.; Susca, L.; Morelli, M., et al. Previsual symptoms of *Xylella fastidiosa* infection revealed in spectral plant trait alterations. *Nat. Plants* 2018, 4, 432-439; DOI:10.1038/s41477-018-0189-7.
86. López-López, M.; Calderón, R.; González-Dugo, V.; Zarco-Tejada, P.; Fereres, E. Early detection and quantification of almond red leaf blotch using high-resolution hyperspectral and thermal imagery. *Remote Sens.* 2016, 8, 276; DOI:10.3390/rs8040276.
87. Omran, E.-S.E. Early sensing of peanut leaf spot using spectroscopy and thermal imaging. *Archives of Agronomy and Soil Science* 2017, 63, 883-896; DOI:10.1080/03650340.2016.1247952.
88. Calderón, R.; Navas-Cortés, J.A.; Zarco-Tejada, P.J. Early detection and quantification of *Verticillium* wilt in olive using hyperspectral and thermal imagery over large areas. *Remote Sens. Environ.* 2015, 7, 5584-5610; DOI:10.3390/rs70505584.
89. Calderón, R.; Navas-Cortés, J.A.; Lucena, C.; Zarco-Tejada, P.J. High-resolution airborne hyperspectral and thermal imagery for early detection of *Verticillium* wilt of olive using fluorescence, temperature and narrow-band spectral indices. *Remote Sens. Environ.* 2013, 139, 231-245; DOI:10.1016/j.rse.2013.07.031.
90. Calderón, R.; Montes-Borrego, M.; Landa, B.; Navas-Cortés, J.; Zarco-Tejada, P. Detection of downy mildew of opium poppy using high-resolution multi-spectral and thermal imagery acquired with an unmanned aerial vehicle. *Precis. Agric.* 2014, 15, 639-661; DOI:10.1007/s11119-014-9360-y.
91. Loladze, A.; Rodrigues, F.A.; Toledo, F.; San Vicente, F.; Gerard, B.; Boddupalli, M.P. Application of remote sensing for phenotyping tar spot complex resistance in maize. *Front. Plant Sci.* 2019, 10, 10; DOI:10.3389/fpls.2019.00552.
92. Zhang, C.Y.; Chen, W.D.; Sankaran, S. High-throughput field phenotyping of *Ascochyta* blight disease severity in chickpea. *Crop Protect.* 2019, 125, 11; DOI:10.1016/j.cropro.2019.104885.

---

Retrieved from <https://encyclopedia.pub/entry/history/show/15392>